

# SCIENTIFIC REPORTS



OPEN

## Formation of xenon-nitrogen compounds at high pressure

Ross T. Howie<sup>1</sup>, Robin Turnbull<sup>2</sup>, Jack Binns<sup>1</sup>, Mungo Frost<sup>2</sup>, Philip Dalladay-Simpson<sup>1</sup> & Eugene Gregoryanz<sup>2</sup>

Received: 06 September 2016

Accepted: 19 September 2016

Published: 17 October 2016

Molecular nitrogen exhibits one of the strongest known interatomic bonds, while xenon possesses a closed-shell electronic structure: a direct consequence of which renders both chemically unreactive. Through a series of optical spectroscopy and x-ray diffraction experiments, we demonstrate the formation of a novel van der Waals compound formed from binary Xe-N<sub>2</sub> mixtures at pressures as low as 5 GPa. At 300 K and 5 GPa Xe(N<sub>2</sub>)<sub>2</sub>-I is synthesised, and if further compressed, undergoes a transition to a tetragonal Xe(N<sub>2</sub>)<sub>2</sub>-II phase at 14 GPa; this phase appears to be unexpectedly stable at least up to 180 GPa even after heating to above 2000 K. Raman spectroscopy measurements indicate a distinct weakening of the intramolecular bond of the nitrogen molecule above 60 GPa, while transmission measurements in the visible and mid-infrared regime suggest the metallisation of the compound at ~100 GPa.

Nitrogen is the most abundant element in the terrestrial atmosphere, existing as a diatomic molecule with one of the strongest known triple bonds and as a result is unreactive at ambient conditions. Under high compression, molecular nitrogen exhibits a rich polymorphism<sup>1–7</sup> and significant overlap of thermodynamically competing phases, dependent on formation conditions<sup>8</sup>. The application of high pressure can also provide new synthesis routes, initiating chemical processes that would not happen otherwise, such as N<sub>2</sub> becoming reactive with the noble metals, as in the formation of platinum or iridium nitrides<sup>9,10</sup>. Xenon, an archetypical inert gas due to its closed shell system, has long been known to form stable halide and oxide compounds through chemical synthesis<sup>11,12</sup>. The reactivity can also be fundamentally altered with the application of high pressure, the process which has produced van der Waals compounds composed of Xe-H<sub>2</sub><sup>13</sup> and Xe-O<sub>2</sub><sup>14</sup>, as well as a Xe-H<sub>2</sub>O clathrate<sup>15</sup>. Direct reactions have also been observed such as that between xenon and ice<sup>16</sup> and the recently reported stable oxides, Xe<sub>2</sub>O<sub>5</sub> and Xe<sub>3</sub>O<sub>2</sub><sup>17</sup>. Xenon has also been shown to be inserted into both quartz<sup>18</sup>, and a small-pore zeolite at high pressure and temperature<sup>19</sup>. Theoretical studies also suggest the increased reactivity of xenon at high pressures with the formation of binary solids Xe-O<sup>20,21</sup>, Xe-Fe/Ni<sup>22</sup>, and Xe-Mg<sup>23</sup> synthesised solely from their constituent elements. Such studies on the reactivity of xenon, especially with terrestrially abundant elements, could provide an explanation into the significant under-abundance of xenon detectable in the Earth's atmosphere.

The direct reaction of N<sub>2</sub> and Xe would seem unlikely due to the relative inertness of both materials. Nevertheless, a recent theoretical study predicts the formation of novel xenon nitride compounds above 146 GPa with stoichiometry - XeN<sub>6</sub><sup>24</sup>. Possible interactions between Xe and N<sub>2</sub> have been explored experimentally at low pressures investigating mutual solubility<sup>25,26</sup>. Through Raman spectroscopic measurements those studies inferred the formation of an orientationally disordered van der Waals compound but were limited up to pressures of 13 GPa at 408 K with no structural investigation.

It is known that at high pressures both xenon and nitrogen exhibit (semi-)conducting phases. Xenon has been shown to transform to metallic state at pressures between 130–150 GPa, giving it the lowest pressure of metallisation amongst the rare gas solids<sup>27–29</sup> and nitrogen becomes semiconducting with band gap of 0.4 eV at 240 GPa<sup>3,3</sup>. Previous studies have claimed that by doping Xe with O<sub>2</sub>, the metallisation pressure is drastically reduced<sup>30</sup>. Therefore it is of significant interest to investigate pressure-induced electronic effects of any formed Xe-N<sub>2</sub> compound. Here, we report the synthesis and characterisation of a Xe-N<sub>2</sub> van der Waals compound through x-ray diffraction, Raman and transmission spectroscopies. We show that two inert condensed gases form a Xe(N<sub>2</sub>)<sub>2</sub> compound at pressures as low as 5 GPa at room temperature. When the novel compound is formed in a xenon medium, it becomes metallic at around 100 GPa, whilst Xe(N<sub>2</sub>)<sub>2</sub> with an abundance of nitrogen demonstrates metallic behaviour above ~140 GPa.

<sup>1</sup>Center for High Pressure Science & Technology Advanced Research, Shanghai, 201203, P.R. China. <sup>2</sup>Centre for Science at Extreme Conditions and School of Physics and Astronomy, University of Edinburgh, Edinburgh, UK. Correspondence and requests for materials should be addressed to R.T.H. (email: ross.howie@hpstar.ac.cn)

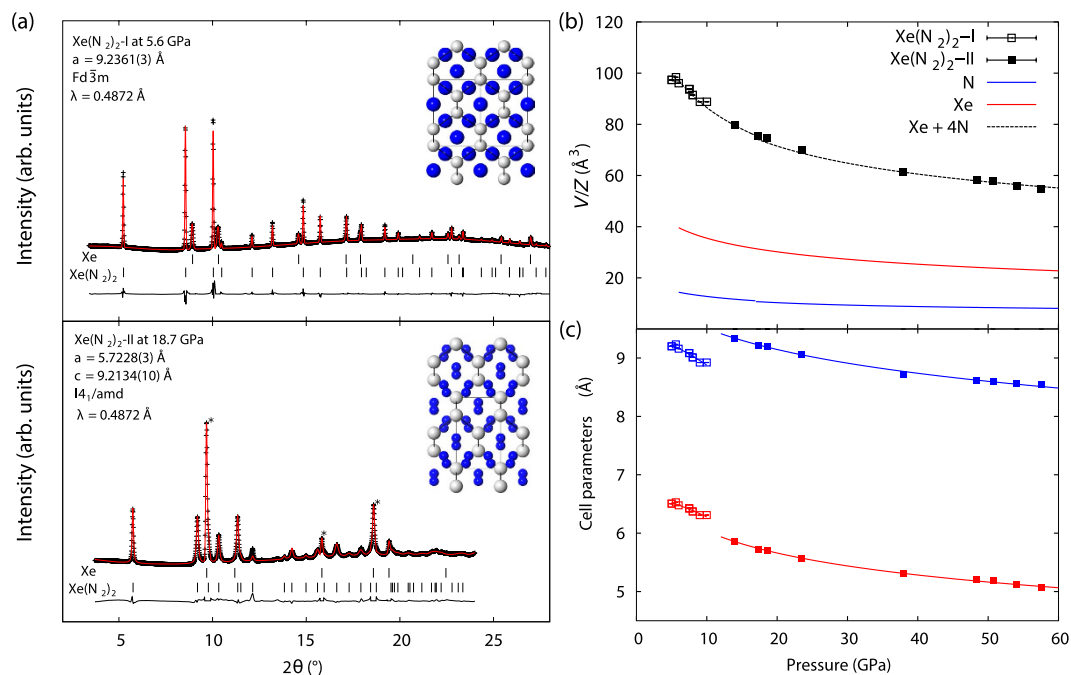


**Figure 1.** (a) Powder X-ray diffraction patterns at 5.6 and 18.7 GPa used for Rietveld refinement. Below 14 GPa,  $\text{Xe}(\text{N}_2)_2$  adopts a face-centered cubic structure, space group  $Fd\bar{3}m$ ,  $a = 9.2361(3)$  Å denoted  $\text{Xe}(\text{N}_2)_2$ -I. At 14 GPa and above  $\text{Xe}(\text{N}_2)_2$  undergoes a transition to a body-centered tetragonal structure,  $I4_1/amd$ , with unit-cell dimensions  $a = 5.7228(3)$ ,  $c = 9.2134(10)$  Å at 18.7 GPa. Peaks corresponding to Xe (marked with \*) were excluded from the profile used in the refinement. Insets show crystal-structure projections for both phases, phase I is rotated to view down the face diagonal  $\langle 110 \rangle$  highlighting structural similarity to phase II. Freely rotating  $\text{N}_2$  molecules in phase I are represented by blue spheres, whilst in phase II blue spheres represent atoms in aligned  $\text{N}_2$  molecules; (b) Equation-of-state data for  $\text{Xe}(\text{N}_2)_2$  compounds. Pressure-volume per Z data for Xe phases is indicated by red lines<sup>32</sup>,  $\text{N}_2$  phases by blue lines<sup>6</sup>. Black squares indicate volume per Z data for  $\text{Xe}(\text{N}_2)_2$  phases I and II, dashed black line indicates the calculated volume for stoichiometry  $\text{Xe} + 4\text{N}$  from atomic volume data; (c) Response of unit-cell dimensions to applied pressure for  $\text{Xe}(\text{N}_2)_2$ , phase I data are shown for unit-cell length  $a$  (blue open squares) and  $d_{(110)}$  (red open squares), phase II data is plotted for unit-cell lengths  $a$  (red closed squares) and  $c$  (blue closed squares). Solid lines indicate fitted linear Birch-Murnaghan linear equations of state?

Mixtures of Xe- $\text{N}_2$  at various concentration were loaded into diamond-anvil cells (DAC) using a combination of cryogenic and high-pressure gas-loading techniques (see Methods section). Compressing the mixture above 2 GPa leads to the formation of a xenon single crystal surrounded by liquid  $\text{N}_2$  as seen visually and in x-ray diffraction measurements (see Figs S1 and S2). At pressures above 5 GPa we observe the formation of a  $\text{N}_2$ -rich compound in the media surrounding the xenon single crystal (Fig. S2). Through x-ray powder diffraction analysis we have identified this phase as having a *fcc* structure, with  $a = 9.2361(3)$  Å at 5.6 GPa (Fig. 1), indexing with space group  $Fd\bar{3}m$  or  $Fd\bar{3}$  accounts for all observed Bragg peaks. Several patterns were of sufficient quality to allow for Rietveld refinement, otherwise Le Bail fitting was used to extract unit-cell dimensions. Solution of the structure by charge-flipping suggests space group  $Fd\bar{3}m$ . Two atomic sites could be refined;  $\text{Xe}(0, 0, 0)$  and  $\text{N}(\frac{5}{8}, \frac{1}{8}, \frac{1}{8})$  resulting in a cubic Laves  $\text{Cu}_2\text{Mg}$ -type structure (Fig. 1(a)).

From both the structure type and unit-cell dimensions we determine the stoichiometry as  $\text{Xe}(\text{N}_2)_2$ , designated  $\text{Xe}(\text{N}_2)_2$ -I herein, which is in excellent agreement with the calculated equation-of-state data for  $\text{Xe} + 4\text{N}$  (Fig. 1(b), see also below). Both the structure type and the stoichiometry are identical to that proposed for oxygen-rich xenon mixtures<sup>14</sup>. The N-N site distances of 3.2655(1) Å are clearly too long to be bonded, these sites therefore represent scattering from disordered  $\text{N}_2$  molecules.  $\text{N}_2$  molecules have been found to adopt both spherical and disk-like rotational disordering in the solid state<sup>31</sup>, and refinement of both disorder types was attempted, with a spherical disorder model (*i.e.* with the N-site occupancy equal to 2) resulting in the best fit to the data (see table in SM for more details on the structure refinement). The structure of this phase can be considered as a diamond-type host lattice of Xe atoms with four rotationally disordered  $\text{N}_2$  molecules forming a tetrahedron within each vacancy. The N-N site distance of 3.2655(1) Å implies a N...N closest-contact distance of 2.1655(1) Å.

Raman spectroscopy measurements of the formed single crystal at 2 GPa reveals the appearance of a weak vibrational mode, which is lower in frequency than the fluid  $\text{N}_2$  vibrational mode by  $10 \text{ cm}^{-1}$  (compare red and black spectra in Fig. 2). This mode has been observed in a previous high-temperature study and attributed to fluid  $\text{N}_2$  dissolved in the Xe crystal lattice<sup>26</sup>. By contrast, in xenon-rich samples (*ca.* 4:1 concentration), we observe the complete transformation of the sample, evident through only the low-frequency vibrational mode and no evidence of excess  $\text{N}_2$  (see SM).

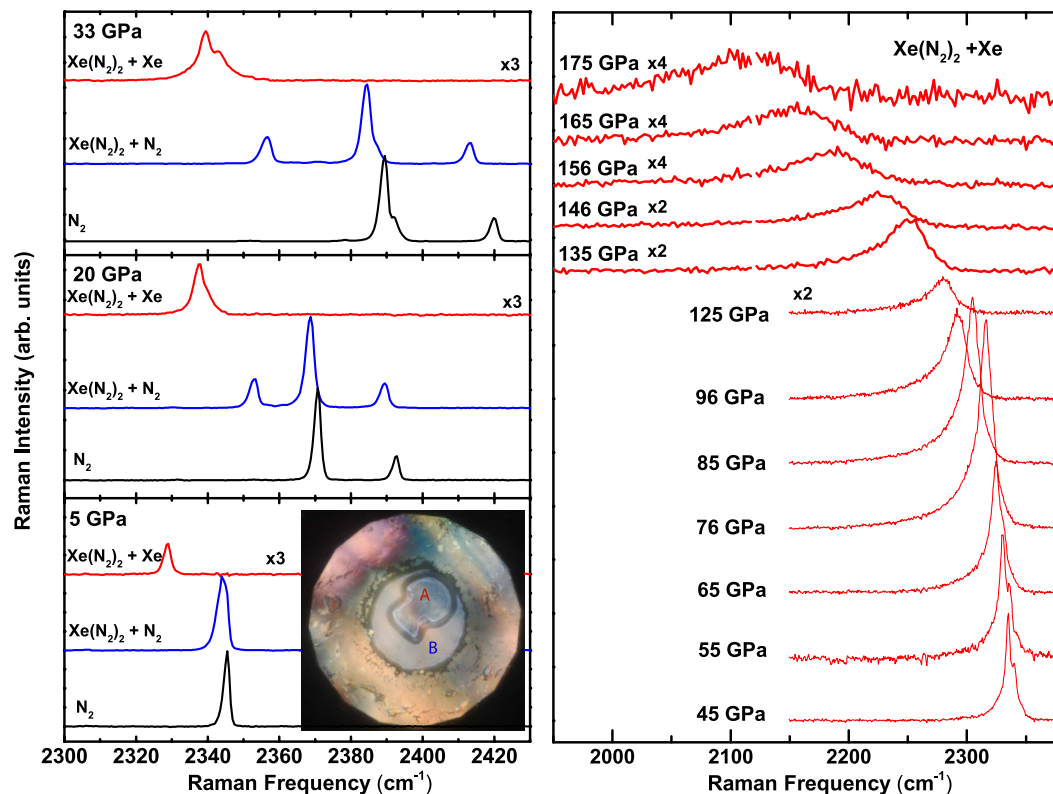


**Figure 2.** (a) Representative vibrational Raman spectra of the Xe-N<sub>2</sub> compound at 5, 20 and 33 GPa. Red spectra are from the formed compound in Xe media, whilst blue spectra show the compound formed in N<sub>2</sub> media. As a comparison, vibrational spectra of pure N<sub>2</sub> are shown in black. Inset: Photomicrograph of sample at 5 GPa. Red spectra were taken at position A in the single crystal and blue spectra were taken in the surrounding medium at position B. (b) Representative vibrational Raman spectra of Xe(N<sub>2</sub>)<sub>2</sub> in a Xe matrix to pressures of 175 GPa.

In Raman measurements of the surrounding media (see blue spectra in Fig. 2), we observe a broad N<sub>2</sub> mode at 5 GPa, which consists of overlapping modes of Xe(N<sub>2</sub>)<sub>2</sub>-I, as determined by x-ray diffraction, and pure N<sub>2</sub> that increasingly separate in frequency space at higher pressure. The vibrational mode of Xe(N<sub>2</sub>)<sub>2</sub>-I (blue spectra in Fig. 2) and the vibrational mode attributed to N<sub>2</sub> in Xe (red spectra in Fig. 2), exhibit identical behaviour with pressure (see red and blue points in Fig. 3a), suggesting that the latter is most likely due to small crystallites of Xe(N<sub>2</sub>)<sub>2</sub>-I that form within a Xe matrix. It should be noted that the presence of this N-containing dopant does not significantly affect the measured unit-cell volume which agrees with the literature to within experimental error<sup>32</sup>.

Above pressures of 14 GPa, we observe a phase transition from the low-pressure Xe(N<sub>2</sub>)<sub>2</sub>-I to a high-pressure Xe(N<sub>2</sub>)<sub>2</sub>-II phase. This transition pressure corresponds approximately to the critical pressure of the  $\delta$  to  $\epsilon$  transition in pure molecular N<sub>2</sub>. Xe(N<sub>2</sub>)<sub>2</sub>-II adopts a body-centered tetragonal cell with  $a = 5.7228(3)$ ,  $c = 9.2134(10)$  Å at 18.7 GPa (Fig. 1). Systematic-absence analysis unambiguously confirm space-group symmetry  $I4_1/amd$ . Again Xe is located at the origin, with one N position refined to (0.5, 0.721(2), 0.179(1)). This position lies displaced by 0.52(2) Å from an inversion centre resulting in four ordered N<sub>2</sub> molecules aligned along the  $c$ -axis. Final Rietveld agreement factors are  $R_p = 0.015$  and  $R = 0.094$ .

The origin of this transition lies in the ordered orientation of N<sub>2</sub> molecules within the vacancy, corroborated by the poorer fit to the data ( $R = 0.1672$ ) with a spherically-disordered N<sub>2</sub> molecule model. Shortest N...N interatomic distances are now 2.5238(1) Å and 2.610(12) Å at 18.7 GPa. Recalling that the shortest N...N interatomic distances at 5.6 GPa were 2.1655(1) Å in phase I, the alignment of N<sub>2</sub> molecules relieves unfavourable close N...N contacts while maintaining the same coordination number for each N<sub>2</sub> molecule.

Over the I-II phase transition the unit cell undergoes a tetragonal distortion elongating by 0.323(3) Å (+3.6%) along  $c$  accompanied by a reduction of  $-0.519(1)$  Å ( $-8.1\%$ ) along tetragonal  $a$ , corresponding to  $\langle 110 \rangle$  in phase I (see table in SM for more details on the structure refinement). We tracked unit-cell dimensions for Xe(N<sub>2</sub>)<sub>2</sub>-II up to 58 GPa (Fig. 1(c)), confirming again the stoichiometry of the compound (Fig. 1(a)) and allowing the determination of equation-of-state parameters for both Xe(N<sub>2</sub>)<sub>2</sub> phases (see methods section). At pressures of 38 GPa and above there were clear signs of the incipient high-pressure  $hcp$  phase of Xe accompanied by strong diffuse scattering and increased background at  $d$ -spacings overlapping with a significant number of Xe(N<sub>2</sub>)<sub>2</sub> reflections and above 58 GPa unit-cell dimensions could not be reliably extracted from the data. However the low-angle (101) reflection could be observed up to 103 GPa (see Fig. S4).

Above 40 GPa, the frequency dependence with pressure of the vibrational mode of Xe(N<sub>2</sub>)<sub>2</sub> deviates greatly from that of pure N<sub>2</sub> (Fig. 3). The maximum in the vibrational frequency vs. pressure is shifted from 80 GPa in pure N<sub>2</sub> to 30 GPa. In the sample in Xe matrix, we observe splitting of the vibrational band (see Fig. 2) up to 70 GPa, after

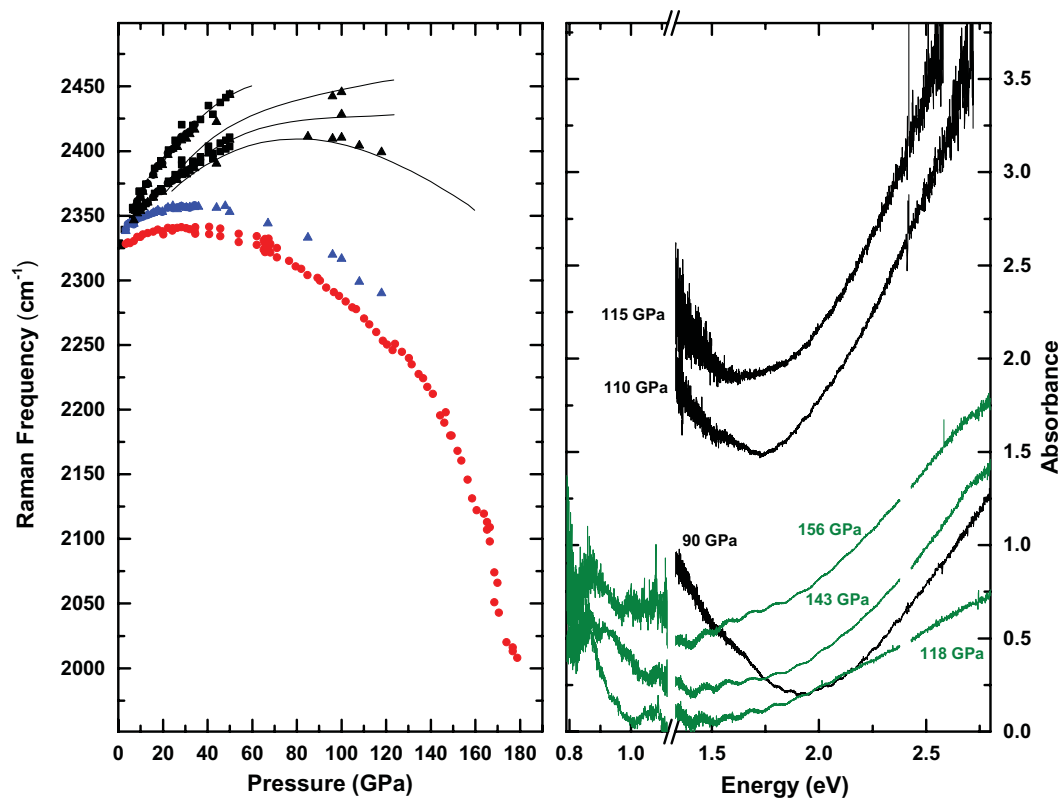


**Figure 3.** Left Panel: Frequencies of the vibrational modes as a function of pressure.  $\text{Xe}(\text{N}_2)_2$  Raman frequencies in Xe medium are shown in red,  $\text{Xe}(\text{N}_2)_2$  Raman frequencies in  $\text{N}_2$  medium are shown in blue and black points are the Raman frequencies of the excess  $\text{N}_2$ . Black lines are taken from a study on pure  $\text{N}_2$ <sup>1</sup>. Right Panel: Optical absorption as a function of energy for Xe-rich (black) and  $\text{N}_2$ -rich (green) samples. The reference spectra were taken at 50 GPa in both experiments.

which the splitting is not distinguishable due to the enhanced broadening of the modes. At 140 GPa the  $\text{N}_2$  vibrational frequencies of  $\text{Xe}(\text{N}_2)_2$  are  $2161\text{ cm}^{-1}$  and  $2212\text{ cm}^{-1}$ , considerably lower frequencies than either those of  $\kappa\text{-N}_2$  ( $2376\text{ cm}^{-1}$ ) or  $\lambda\text{-N}_2$  ( $2320\text{ cm}^{-1}$ ,  $2400\text{ cm}^{-1}$ ). Interestingly, at 178 GPa, we observe the persistence of molecular nitrogen, which is above the pressure at which pure  $\text{N}_2$  is claimed to become non-molecular ( $\eta\text{-N}_2$ )<sup>1–3</sup>. We note that although we observe a much softer  $\text{N}_2$  molecular mode than that just before  $\zeta$  transforms to the non-molecular amorphous  $\eta$  phase in pure  $\text{N}_2$ , there is no evidence that the  $\text{N}_2$  molecules in  $\text{Xe}(\text{N}_2)_2$  dissociate to form Xe-N bonding. However, there is a clear reduction in intensity (see Fig. 2) together with a marked increase in the FWHM (see Fig. S5) indicating that the molecular N-N bond is weakening. Up to highest pressure studied (180 GPa) we see no evidence of Xe-N bonded compounds predicted by theory<sup>24</sup>. In an attempt to promote synthesis of such compounds, we performed laser heating of the sample to temperatures of 3000 K at 120, 150, 160 and 180 GPa but no transition was observed in either Raman spectroscopy or x-ray diffraction. It is remarkable that a van der Waals solid, the components of which are inert materials, can remain stable to such extreme conditions.

Figure 3(b) shows the transmission spectra collected from two samples with different initial ratio of Xe and  $\text{N}_2$ . The spectra were collected with both visible and mid infrared light sources which allow the coverage of energy region between  $\sim 3$  to 0.6 eV. The samples in a Xe matrix (black), appear to exhibit metallic behaviour evident by the sharp rise in the absorption in the near-IR, which shifts with pressure. By 120 GPa, no detectable transmission was observed in the visible, the sample appearance became shiny and reflected red laser light (see photomicrographs in Fig. S6). Samples of  $\text{Xe}(\text{N}_2)_2$  with higher  $\text{N}_2$  concentrations do exhibit absorption (Fig. 3 green) but not to the same extent as in the Xe matrix, which could be due to the excess of  $\text{N}_2$ . Pure xenon has been shown to be conductive at above 135 GPa through both absorption/reflectivity and electrical measurements<sup>27–29</sup>. The mechanism of conductivity is an indirect overlap of the  $5p$  valence and  $5d$  conduction bands. Although determining the mechanism was beyond the scope of this study, our results indicate that by doping Xe with  $\text{N}_2$ , or  $\text{Xe}(\text{N}_2)_2$ , we are able to tune the conductive properties of Xe and lower the pressure of metallisation.

Our results demonstrate that xenon can form compounds not only with chemically reactive gases such as hydrogen or oxygen, but also with unreactive nitrogen. That such a compound forms at low pressure, exhibits metallic properties, and stable to both high-pressure and high-temperature conditions will no doubt stimulate further research in the reactivity of xenon, an element which now appears to be substantially less inert than previously thought.

## Methods

We have studied the formation conditions and stability of xenon and nitrogen compounds up to pressures of 180 GPa in a diamond anvil cell (DAC). In total 12 DAC loadings were performed. 200  $\mu\text{m}$  culet flat diamonds were used for experiments under 50 GPa, while 60  $\mu\text{m}$  and 150  $\mu\text{m}$  culets were used for higher pressure experiments. In all experiments rhenium foil was used as the gasket material.

The loading of the Xe-N<sub>2</sub> consisted of two stages. Solid Xe (99.9% purity) was initially cryogenically loaded into a DAC under a N<sub>2</sub> atmosphere. Loading was confirmed initially through comparisons of white light transmission spectra due to the change in refractive index between the empty sample chamber and loaded sample. Thorough mapping of the sample with Raman spectroscopy was carried out to ensure no impurities were present in the sample and further confirmation was obtained through x-ray diffraction analysis.

N<sub>2</sub> gas (99.9% purity) was then loaded into the cell at a pressure of 20 MPa using a high-pressure gas loading system, displacing some of the pre-existing Xe gas. The volume ratio was estimated by the phase separation of Xe and N<sub>2</sub> in the fluid state. Using a combination of varying pressure and temperature, single crystals of the Xe rich mixture were grown.

We have used 514 and 647 nm as excitation wavelengths in the Raman spectroscopy measurements using a custom-built micro-focussed Raman system. Pressure was determined through both ruby fluorescence ( $P < 100$  GPa) and the Raman edge of the stressed diamond<sup>33</sup>.

Powder x-ray diffraction data were collected at several beamlines: BL10XU at Spring-8 (Japan), IDB PETRA-III (Germany), ID09 at the European Synchrotron Radiation Facility (France), and ID-BMD of HPCAT at APS (USA). Incident beam energies in the range 25–30 keV were used. Intensity vs.  $2\theta$  plots were obtained by integrating image plate data in various formats using DIOPTAS<sup>34</sup>. Indexing was carried out in GSAS-II<sup>35</sup>, Le Bail and Rietveld refinements were carried out in Jana2000<sup>36</sup>. Equation of state data were determined using EoSFIT 7<sup>37</sup>. Fitted equation of state parameters for Xe(N<sub>2</sub>)<sub>2</sub>-I:  $V_0 = 873(90) \text{ \AA}^3$ ,  $K_0 = 47(56) \text{ GPa}$ ,  $K' = 1(5)$ . Equation-of-state parameters for Xe(N<sub>2</sub>)<sub>2</sub>-II:  $V_0 = 526(158) \text{ \AA}^3$ ,  $K_0 = 9(14) \text{ GPa}$ ,  $K' = 4.5(11)$ ,  $K'' = -0.51131 \text{ GPa}^{-1}$ .

## References

- Goncharov, A., Gregoryanz, E., Mao, H., Liu, Z. & Hemley, R. Optical evidence for a non-molecular phase of nitrogen above 150 gpa. *Phys. Rev. Lett.* **85**, 1262–1265 (2000).
- Eremets, M. I., Hemley, R. J., Mao, H.-k. & Gregoryanz, E. Semiconducting non-molecular nitrogen up to 240 gpa and its low-pressure stability. *Nature* **411**, 170–174 (2001).
- Gregoryanz, E., Goncharov, A. F., Hemley, R. J. & Mao, H.-k. High-pressure amorphous nitrogen. *Phys. Rev. B* **64**, 052103 (2001).
- Gregoryanz, E. *et al.* Raman, infrared, and x-ray evidence for new phases of nitrogen at high pressures and temperatures. *Phys. Rev. B* **66**, 224108 (2002).
- Eremets, M. I., Gavriluk, A. G., Trojan, I. A., Dzivenko, D. A. & Boehler, R. Single-bonded cubic form of nitrogen. *Nat. Mater.* **3**, 558–563 (2004).
- Gregoryanz, E. *et al.* High p-t transformations of nitrogen to 170 gpa. *J. Chem. Phys.* **126**, 184505 (2007).
- Tomasino, D., Kim, M., Smith, J. & Yoo, C.-S. Pressure-induced symmetry-lowering transition in dense nitrogen to layered polymeric nitrogen (lp-n) with colossal raman intensity. *Phys. Rev. Lett.* **113**, 205502 (2014).
- Frost, M., Howie, R. T., Dalladay-Simpson, P., Goncharov, A. F. & Gregoryanz, E. Novel high-pressure nitrogen phase formed by compression at low temperature. *Phys. Rev. B* **93**, 024113 (2016).
- Gregoryanz, E. *et al.* Synthesis and characterization of a binary noble metal nitride. *Nat. Mater.* **3**, 294–297 (2004).
- Young, A. *et al.* Synthesis of novel transition metal nitrides IrN<sub>2</sub> and OsN<sub>2</sub>. *Phys. Rev. Lett.* **96**, 155501 (2006).
- Bartlett, N. Xenon hexafluoroplatinate(v)  $\text{Xe} + [\text{PtF}_6]$ . *Proc. Chem. Soc.* **218** (1962).
- Classen, H. H., Selig, H. & Malm, J. G. Xenon tetrafluoride. *J. Am. Phys. Soc.* **84**, 3593–3593 (1962).
- Somayazulu, M. *et al.* Pressure-induced bonding and compound formation in xenon-hydrogen solids. *Nat. Chem.* **2**, 50–53 (2009).
- Weck, G., Dewaele, A. & Loubeyre, P. Oxygen/noble gas binary phase diagrams at 296 K and high pressures. *Phys. Rev. B* **82**, 014112 (2010).
- Sanloup, C., Mao, H.-k. & Hemley, R. J. High-pressure transformations in xenon hydrates. *P. Natl. Acad. Sci.* **99**, 25–28 (2001).
- Sanloup, C., Bonev, S. A., Hochlaf, M. & Maynard-Casely, H. E. Reactivity of xenon with ice at planetary conditions. *Phys. Rev. Lett.* **110**, 1–5 (2013).
- Dewaele, A. *et al.* Synthesis and stability of xenon oxides Xe<sub>2</sub>O<sub>5</sub> and Xe<sub>3</sub>O<sub>2</sub> under pressure. *Nat. Chem.* advance online publication (2016).
- Sanloup, C. *et al.* Retention of xenon in quartz and earth's missing xenon. *Science* **310**, 1174–1177 (2005).
- Seoung, S. *et al.* Irreversible xenon insertion into a small-pore zeolite at moderate pressures and temperatures. *Nat. Chem.* **6**, 835 (2014).
- Brock, D. S. & Schrobilgen, G. J. Synthesis of the missing oxide of xenon, XeO<sub>2</sub>, and its implications for earth's missing xenon. *J. Am. Chem. Soc.* **133**, 6265–6269 (2011).
- Zhu, Q. *et al.* Stability of xenon oxides at high pressures. *Nat. Chem.* **5**, 61–65 (2012).
- Zhu, L., Liu, H., Pickard, C. J., Zou, G. & Ma, Y. Reactions of xenon with iron and nickel are predicted in the earth's inner core. *Nat. Chem.* **6**, 644–648 (2014).
- Miao, M.-s. *et al.* Anionic chemistry of noble gases: Formation of mg-ng (ng = xe, kr, ar) compounds under pressure. *J. Am. Chem. Soc.* **137**, 14122–14128 (2015).
- Peng, F., Wang, Y., Wang, H., Zhang, Y. & Ma, Y. Stable xenon nitride at high pressures. *Phys. Rev. B* **92**, 094104 (2015).
- Kooi, M. E. & Schouten, J. A. High-pressure raman investigation of mutual solubility and compound formation in Xe N<sub>2</sub> and Ne N<sub>2</sub>. *Phys. Rev. B* **60**, 12635–12643 (1999).
- Kooi, M. E., Michels, J. P. J. & Schouten, J. A. Negative vibrational shift of nitrogen diluted in xenon at the fluid-solid transition. *J. Chem. Phys.* **110**, 3023–3025 (1999).
- Reichlin, R. *et al.* Evidence for the insulator-metal transition in xenon from optical, x-ray, and band-structure studies to 170 gpa. *Phys. Rev. Lett.* **62**, 669–672 (1989).
- Goettel, K. A., Eggert, J. H., Silvera, I. F. & Moss, W. C. Optical evidence for the metallization of xenon at 132(5) gpa. *Phys. Rev. Lett.* **62**, 665–668 (1989).
- Eremets, M. *et al.* Electrical conductivity of xenon at megabar pressures. *Phys. Rev. Lett.* **85**, 2797–2800 (2000).
- Dewaele, A., Loubeyre, P., Dumas, P. & Mezouar, M. Oxygen impurities reduce the metallization pressure of xenon. *Phys. Rev. B* **86**, 014103 (2012).
- Hanfland, M. *et al.* Structures of molecular nitrogen at high pressures. *The Review of High Pressure Science and Technology* **7**, 787–789 (1998).

32. Cynn, H. *et al.* Martensitic fcc-to-hcp transformation observed in xenon at high pressure. *Phys. Rev. Lett.* **86**, 4552–4555 (2001).
33. Akahama, Y. & Kawamura, H. Pressure calibration of diamond anvil raman gauge to 410 gpa. *J. Phys.: Conf. Ser.* **215**, 012195 (2010).
34. Prescher, C. & Prakapenka, V. B. Dioptas: a program for reduction of two-dimensional x-ray diffraction data and data exploration. *High Pressure Res.* **35**, 223–230 (2015).
35. Toby, B. H. & Von Dreele, R. B. GSAS-II: the genesis of a modern open-source all purpose crystallography software package. *J. Appl. Crystallogr.* **46**, 544–549 (2013).
36. Petříček, V., Dušek, M. & Palatinus, L. Crystallographic computing system jana2006: general features. *Z. Kristallogr.* **229**, 345–352 (2014).
37. Gonzalez-Platas, J., Alvaro, M., Nestola, F. & Angel, R. EosFit7-GUI: a new graphical user interface for equation of state calculations, analyses and teaching. *J. Appl. Crystallogr.* **49**, 1377–1382 (2016).

## Acknowledgements

Synchrotron radiation experiments were performed at the BL10XU of SPring-8 with the approval of the Japan Synchrotron Radiation Research Institute (JASRI) (Proposal No. 2016A1041), the authors would like to acknowledge Saori Imada and Naohisa Hirao for assistance with experiments. We acknowledge the European Synchrotron Radiation Facility for provision of synchrotron radiation facilities and we would like to thank Micheal Hanfland for assistance in using beamline ID09. Parts of this research were carried out at the light source PETRA III at DESY, a member of the Helmholtz Association (HGF). We would like to thank Konstantin Glazyrin for assistance in using beamline IDB. This research used resources of the Advanced Photon Source, a U.S. Department of Energy (DOE) Office of Science User Facility operated for the DOE Office of Science by Argonne National Laboratory under Contract No. DE-AC02-06CH11357. Part of this work were performed at HPCAT (Sector 16), Advanced Photon Source (APS), Argonne National Laboratory (ANL), we would like to thank Changyong Park for assistance with experiments. This work was supported by a research grant from the U.K. EPSRC Leadership Fellowship grant EP/J003999/1.

## Author Contributions

R.T.H. conceived and designed the project, carried out the experiments, analysed the data and wrote the paper. R.T. and J.B. carried out the experiments, analysed the data and wrote the paper. M.F. and P.D.-S. carried out the experiments. E.G. analysed the data and wrote the paper.

## Additional Information

**Supplementary information** accompanies this paper at <http://www.nature.com/srep>

**Competing financial interests:** The authors declare no competing financial interests.

**How to cite this article:** Howie, R. T. *et al.* Formation of xenon-nitrogen compounds at high pressure. *Sci. Rep.* **6**, 34896; doi: 10.1038/srep34896 (2016).



This work is licensed under a Creative Commons Attribution 4.0 International License. The images or other third party material in this article are included in the article's Creative Commons license, unless indicated otherwise in the credit line; if the material is not included under the Creative Commons license, users will need to obtain permission from the license holder to reproduce the material. To view a copy of this license, visit <http://creativecommons.org/licenses/by/4.0/>

© The Author(s) 2016